NUCL SCI TECH (2021) 32:117
https://doi.org/10.1007/s41365-021-00955-2

Basic quantities of the equation of state in isospin asymmetric nuclear matter

Jie Liu[1] · Chao Gao[1] · Niu Wan[2] · Chang Xu[1]

Received: 11 May 2021 / Revised: 15 August 2021 / Accepted: 16 August 2021 / Published online: 30 October 2021

Abstract Based on the Hugenholtz–Van Hove theorem, six basic quantities of the EoS in isospin asymmetric nuclear matter are expressed in terms of the nucleon kinetic energy $t(k)$, the isospin symmetric and asymmetric parts of the single-nucleon potentials $U_0(\rho,k)$ and $U_{\mathrm{sym,i}}(\rho,k)$. The six basic quantities include the quadratic symmetry energy $E_{\mathrm{sym,2}}(\rho)$, the quartic symmetry energy $E_{\mathrm{sym,4}}(\rho)$, their corresponding density slopes $L_2(\rho)$ and $L_4(\rho)$, and the incompressibility coefficients $K_2(\rho)$ and $K_4(\rho)$. By using four types of well-known effective nucleon–nucleon interaction models, namely the BGBD, MDI, Skyrme, and Gogny forces, the density- and isospin-dependent properties of these basic quantities are systematically calculated and their values at the saturation density ρ_0 are explicitly given. The contributions to these quantities from $t(k)$, $U_0(\rho,k)$, and $U_{\mathrm{sym,i}}(\rho,k)$ are also analyzed at the normal nuclear density ρ_0. It is clearly shown that the first-order asymmetric term $U_{\mathrm{sym,1}}(\rho,k)$ (also known as the symmetry potential in the Lane potential) plays a vital role in determining the density dependence of the quadratic symmetry energy $E_{\mathrm{sym,2}}(\rho)$. It is also shown that the contributions from the high-order asymmetric parts of the single-nucleon potentials ($U_{\mathrm{sym,i}}(\rho,k)$ with $i>1$) cannot be neglected in the calculations of the other five basic quantities. Moreover, by analyzing the properties of asymmetric nuclear matter at the exact saturation density $\rho_{\mathrm{sat}}(\delta)$, the corresponding quadratic incompressibility coefficient is found to have a simple empirical relation $K_{\mathrm{sat,2}} = K_2(\rho_0) - 4.14L_2(\rho_0)$.

Keywords Equation of state · Symmetry energy · HVH theorem · Single-nucleon potential

This work was supported by the National Natural Science Foundation of China (No. 11822503).

✉ Chang Xu
cxu@nju.edu.cn

[1] School of Physics, Nanjing University, Nanjing 210093, China

[2] School of Physics and Optoelectronics, South China University of Technology, Guangzhou 510641, China

1 Introduction

Research on the isospin- and density-dependent properties of the equation of state (EoS) in isospin asymmetric nuclear matter is a longstanding issue in both nuclear physics and astrophysics [1–4]. With respect to the exchange symmetry between protons and neutrons, the EoS for asymmetric nuclear matter can be expressed as an even series of isospin asymmetry $E(\rho,\delta) = E_0(\rho) + \sum_{i=2,4,\ldots} E_{\mathrm{sym,i}}(\rho)\delta^i$, in which the first term is the energy per nucleon in symmetric nuclear matter and the coefficients of the isospin-dependent terms are known as the i-th order symmetry energy $E_{\mathrm{sym,i}}(\rho) = \frac{1}{i!}\frac{\partial^i E(\rho,\delta)}{\partial\delta^i}|_{\delta=0}$. In recent years, the EoS of nuclear matter has been extensively studied by (I) microscopic and phenomenological many-body approaches [5–8]; (II) the observables from heavy-ion reactions [9–14]; (III) the astrophysical observations [15–17]. For symmetric nuclear matter, the saturation density is constrained in a relatively narrow region $\rho_0 = 0.145 \sim 0.180\ \mathrm{fm}^{-3}$ and the corresponding energy per nucleon $E_0(\rho_0)$ is approximately -16 MeV [18]. The incompressibility coefficient $K_0(\rho_0)$ has a generally accepted value of 240 ± 20 MeV constrained by both theoretical approaches and giant monopole resonance data [19–21]. In addition, the skewness $J_0(\rho_0)$ was recently found to have significant effects on the structures of neutron stars, but its value is scattered widely from -800 MeV to 400 MeV [22–24]. For asymmetric nuclear matter, the value of the quadratic symmetry energy $E_{\mathrm{sym},2}(\rho_0)$ is constrained to be 31.7 ± 3.2 MeV [25, 26]. However, its density slope and incompressibility coefficient remain uncertain, that is, $L_2(\rho_0) = 58.7 \pm 28.1$ MeV [25, 26] and $K_{\mathrm{sat},2} = -550 \pm 100$ [27–29]. It should be emphasized that at both sub-saturation and supra-saturation densities, the quadratic symmetry energy is not well constrained, especially at supra-saturation densities [30–33]. The quartic symmetry energy $E_{\mathrm{sym},4}(\rho_0)$ is predicted to be less than 1 MeV [34–36]. In contrast to the quadratic ones, few studies have been conducted on the quartic density slope $L_4(\rho_0)$ and the corresponding incompressibility coefficient $K_4(\rho_0)$ [37].

In the present work, we perform a systematic analysis of six basic quantities in the EoS based on the Hugenholtz–Van Hove (HVH) theorem [38], namely $E_{\mathrm{sym},2}(\rho)$, $E_{\mathrm{sym},4}(\rho)$, $L_2(\rho)$, $L_4(\rho)$, $K_2(\rho)$, and $K_4(\rho)$. Among them, the properties of $E_{\mathrm{sym},2}(\rho)$, $E_{\mathrm{sym},4}(\rho)$, and their slopes $L_2(\rho)$ and $L_4(\rho)$ were re-analyzed [39–43]. The analytical expressions of the incompressibility coefficients $K_2(\rho)$ and $K_4(\rho)$ in terms of single-nucleon potentials are given for the first time. In the literature, there are various effective interaction models: transport models such as the Bombaci–Gale–Bertsch–Das Gupta (BGBD) interaction [44–47], the isospin- and momentum-dependent MDI interaction [47–50], the Lanzhou quantum molecular dynamics (LQMD) model [51–53], and the self-consistent mean-field approach including the zero-range momentum-dependent Skyrme interaction [54–56], the finite-range Gogny interaction [57–59], and the relativistic mean-field model [60, 61]. The values of these quantities at the saturation density ρ_0 are calculated using two types of BGBD interactions: the MDI interactions with $x = -1$, 0 and 1, 16 sets of the Skyrme interactions [62–72], and 4 sets of Gogny interactions [73–75]. By taking the NRAPR Skyrme interaction as an example, we show the isospin- and density-dependent properties of the EoS for asymmetric nuclear matter explicitly. Meanwhile, for symmetric nuclear matter, $E_0(\rho)$, $K_0(\rho)$, and $J_0(\rho)$ are also analyzed in detail. It should be emphasized that the skewness $J_0(\rho_0)$ was recently found to be closely related to not only the maximum mass of neutron stars but also the radius of canonical neutron stars, and the calculations of $J_0(\rho)$ in the present work might be helpful in further determining the properties of neutron stars. In particular, the contributions from the high-order terms of the single-nucleon potential $U_{\mathrm{sym},3}(\rho, k)$ and $U_{\mathrm{sym},4}(\rho, k)$ to these basic quantities are evaluated in detail.

The paper is organized as follows. In Sect. 2, based on the HVH theorem, we express the basic quantities of the EoS in terms of the nucleon kinetic energy and the symmetric and asymmetric parts of the single-nucleon potential. The isospin-dependent saturation properties of the asymmetric nuclear matter are also discussed. In Sect. 3, the calculated results by using four different effective interaction models are given. Finally, a summary is presented in Sect. 4.

2 Decomposition of basic quantities of EoS in terms of global optical potential components

2.1 Basic quantities in the Equation of State of asymmetric nuclear matter

For isospin asymmetric nuclear matter, the EoS can be expanded as a series of isospin asymmetry $\delta = (\rho_{\mathrm{n}} - \rho_{\mathrm{p}})/\rho$. If the high-order terms are neglected, the EoS can be expressed as $E(\rho, \delta) = E_0(\rho) + E_{\mathrm{sym},2}(\rho)\delta^2 + E_{\mathrm{sym},4}(\rho)\delta^4$ (see Fig. 1). Each term can be further expanded around the saturation density of symmetric nuclear matter ρ_0 as a series of dimensionless variables $\chi = \frac{\rho - \rho_0}{3\rho_0}$, which characterizes the deviations of the nuclear density ρ from ρ_0. The density slope and incompressibility coefficient of the i-th order symmetry energy are defined as $L_i(\rho) = 3\rho \frac{\partial E_{\mathrm{sym,i}}(\rho)}{\partial \rho}$ and $K_i(\rho) = 9\rho^2 \frac{\partial^2 E_{\mathrm{sym,i}}(\rho)}{\partial \rho^2}$, respectively. The skewness of the EoS for symmetric nuclear matter is given by $J_0(\rho) = 27\rho^3 \frac{\partial^3 E_0(\rho)}{\partial \rho^3}$.

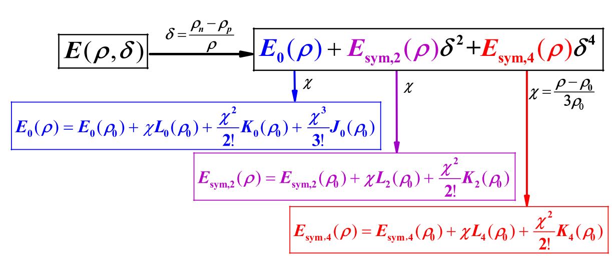

Fig. 1 (Color online) The schematic diagram of basic quantities of the EoS in both isospin symmetric and asymmetric nuclear matter, including $E_0(\rho)$, $E_{\mathrm{sym},2}(\rho)$, $E_{\mathrm{sym},4}(\rho)$, $K_0(\rho_0)$, $J_0(\rho_0)$, $L_2(\rho_0)$, $K_2(\rho_0)$, $L_4(\rho_0)$, and $K_4(\rho_0)$

2.2 The Hugenholtz–Van Hove (HVH) theorem and decomposition of basic quantities of asymmetric nuclear matter

Relating the Fermi energy E_F and the energy per nucleon E, the general Hugenholtz–Van Hove (HVH) theorem can be written as [38]

$$E_F = \frac{d\xi}{d\rho} = E + \rho\frac{dE}{d\rho} = E + \frac{P}{\rho}, \tag{1}$$

where $\xi = \rho E$ and $P = \rho^2 \frac{\partial E}{\partial \rho}$ are the energy density and pressure of the fermion system at an absolute temperature of zero. Accordingly, the Fermi energies of neutrons and protons in asymmetric nuclear matter can be expressed as [41]:

$$t(k_F^n) + U_n(\rho, \delta, k_F^n) = \frac{\partial \xi}{\partial \rho_n}, \tag{2a}$$

$$t(k_F^p) + U_p(\rho, \delta, k_F^p) = \frac{\partial \xi}{\partial \rho_p}, \tag{2b}$$

where $t(k_F^{n/p})$ and $U_{n/p}(\rho, \delta, k_F^{n/p})$ are the kinetic energy and the single-nucleon potential of the neutron/proton with the Fermi momentum $k_F^{n/p} = k_F(1+\tau\delta)^{1/3}$. Furthermore, $U_{n/p}(\rho, \delta, k)$ can be expanded by a series of isospin asymmetries δ as

$$\begin{aligned} U_{n/p}(\rho, \delta, k) =& U_0(\rho, k) + U_{sym,1}(\rho, k)\tau\delta \\ &+ U_{sym,2}(\rho, k)(\tau\delta)^2 + U_{sym,3}(\rho, k)(\tau\delta)^3 \\ &+ U_{sym,4}(\rho, k)(\tau\delta)^4, \end{aligned} \tag{3}$$

where $\tau = 1$ is for the neutron and $\tau = -1$ for the proton, and $U_0(\rho, k)$ and $U_{sym,i}(\rho, k)$ are the symmetric and asymmetric parts, respectively. In particular, $U_0(\rho, k)$ and $U_{sym,1}(\rho, k)$ are called isoscalar and isovector (symmetry) potentials in the popular Lane potential [76].

By subtracting Eq. (2b) from Eq. (2a), we obtain:

$$[t(k_F^n) - t(k_F^p)] + [U_n(\rho, \delta, k_F^n) - U_p(\rho, \delta, k_F^p)] = \frac{\partial \xi}{\partial \rho_n} - \frac{\partial \xi}{\partial \rho_p}. \tag{4}$$

Expressing both sides of Eq. (4) in terms of δ and comparing the coefficients of δ and δ^3, we can obtain the general expressions of the quadratic and quartic symmetry energies as

$$E_{sym,2}(\rho) = \frac{1}{6}\frac{\partial[t(k) + U_0(\rho, k)]}{\partial k}\bigg|_{k_F} k_F + \frac{1}{2}U_{sym,1}(\rho, k_F), \tag{5a}$$

$$\begin{aligned} E_{sym,4}(\rho) =& \frac{5}{324}\frac{\partial[t(k) + U_0(\rho, k)]}{\partial k}\bigg|_{k_F} k_F - \frac{1}{108}\frac{\partial^2[t(k) + U_0(\rho, k)]}{\partial k^2}\bigg|_{k_F} \\ & k_F^2 + \frac{1}{648}\frac{\partial^3[t(k) + U_0(\rho, k)]}{\partial k^3}\bigg|_{k_F} \\ & k_F^3 - \frac{1}{36}\frac{\partial U_{sym,1}(\rho, k)}{\partial k}\bigg|_{k_F} k_F + \frac{1}{72}\frac{\partial^2 U_{sym,1}(\rho, k)}{\partial k^2}\bigg|_{k_F} \\ & k_F^2 + \frac{1}{12}\frac{\partial U_{sym,2}(\rho, k)}{\partial k}\bigg|_{k_F} k_F + \frac{1}{4}U_{sym,3}(\rho, k_F). \end{aligned} \tag{5b}$$

By adding Eqs. (2a) to (2b), expanding both sides of this summation in terms of δ, and comparing the coefficients of δ^0, we can obtain an important relationship between $E_0(\rho)$ and its density slope $L_0(\rho)$

$$E_0(\rho) + \rho\frac{\partial E_0(\rho)}{\partial \rho} = t(k_F) + U_0(\rho, k_F), \tag{6}$$

where $L_0(\rho)$ is defined as $3\rho\frac{\partial E_0(\rho)}{\partial \rho}$ and can be rewritten as

$$L_0(\rho) = 3[t(k_F) + U_0(\rho, k_F)] - 3E_0(\rho). \tag{7}$$

Obviously, $E_0(\rho_0) = t(k_F) + U_0(\rho_0, k_F)$ and $E_0(\rho)$ can be calculated from the energy density of the symmetric nuclear matter $\xi(\rho, \delta = 0)$. Simultaneously, the general expressions of the density slopes $L_2(\rho)$ and $L_4(\rho)$ can also be given by comparing the coefficients of δ^2 and δ^4, namely

$$\begin{aligned} L_2(\rho) =& \frac{1}{6}\frac{\partial[t(k) + U_0(\rho, k)]}{\partial k}\bigg|_{k_F} k_F + \frac{1}{6}\frac{\partial^2[t(k) + U_0(\rho, k)]}{\partial k^2}\bigg|_{k_F} k_F^2 \\ & + \frac{\partial U_{sym,1}(\rho, k)}{\partial k}\bigg|_{k_F} k_F + \frac{3}{2}U_{sym,1}(\rho, k_F) + 3U_{sym,2}(\rho, k_F), \end{aligned} \tag{8a}$$

$$\begin{aligned} L_4(\rho) =& \frac{5}{324}\frac{\partial[t(k) + U_0(\rho, k)]}{\partial k}\bigg|_{k_F} k_F - \frac{1}{324}\frac{\partial^2[t(k) + U_0(\rho, k)]}{\partial k^2}\bigg|_{k_F} k_F^2 \\ & - \frac{1}{216}\frac{\partial^3[t(k) + U_0(\rho, k)]}{\partial k^3}\bigg|_{k_F} k_F^3 + \frac{1}{648}\frac{\partial^4[t(k) + U_0(\rho, k)]}{\partial k^4}\bigg|_{k_F} k_F^4 \\ & - \frac{7}{108}\frac{\partial U_{sym,1}(\rho, k)}{\partial k}\bigg|_{k_F} k_F + \frac{1}{72}\frac{\partial^2 U_{sym,1}(\rho, k)}{\partial k^2}\bigg|_{k_F} k_F^2 \\ & + \frac{1}{54}\frac{\partial^3 U_{sym,1}(\rho, k)}{\partial k^3}\bigg|_{k_F} k_F^3 \\ & + \frac{5}{12}\frac{\partial U_{sym,2}(\rho, k)}{\partial k}\bigg|_{k_F} k_F + \frac{1}{6}\frac{\partial^2 U_{sym,2}(\rho, k)}{\partial k^2}\bigg|_{k_F} k_F^2 \\ & + \frac{\partial U_{sym,3}(\rho, k)}{\partial k}\bigg|_{k_F} k_F + \frac{9}{4}U_{sym,3}(\rho, k_F) + 3U_{sym,4}(\rho, k_F). \end{aligned} \tag{8b}$$

Taking the derivative of the summation of Eqs. (2a) and (2b) with respect to ρ and comparing the coefficients, the incompressibility coefficients of $E_0(\rho)$, $E_{sym,2}(\rho)$, and $E_{sym,4}(\rho)$ are given as

$$K_0(\rho) = 9\rho\frac{\partial[t(k_F)+U_0(\rho,k_F)]}{\partial\rho} - 18[t(k_F) + U_0(\rho,k_F)] + 18E_0(\rho), \tag{9a}$$

$$\begin{aligned}K_2(\rho) = &-\frac{1}{3}\frac{\partial[t(k)+U_0(\rho,k)]}{\partial k}\bigg|_{k_F} k_F + \frac{1}{3}\frac{\partial^2[t(k)+U_0(\rho,k)]}{\partial k^2}\bigg|_{k_F} k_F^2 \\ &- k_F\rho\frac{\partial}{\partial\rho}\frac{\partial[t(k)+U_0(\rho,k)]}{\partial k}\bigg|_{k_F} + \frac{1}{2}k_F^2\rho\frac{\partial}{\partial\rho}\frac{\partial^2[t(k)+U_0(\rho,k)]}{\partial k^2}\bigg|_{k_F} \\ &+ \frac{\partial U_{sym,1}(\rho,k)}{\partial k}\bigg|_{k_F} k_F + 3k_F\rho\frac{\partial}{\partial\rho}\frac{\partial U_{sym,1}(\rho,k)}{\partial k}\bigg|_{k_F} \\ &+ 9\rho\frac{\partial U_{sym,2}(\rho,k_F)}{\partial\rho},\end{aligned} \tag{9b}$$

$$\begin{aligned}K_4(\rho) = &-\frac{5}{162}\frac{\partial[t(k)+U_0(\rho,k)]}{\partial k}\bigg|_{k_F} k_F + \frac{23}{162}\frac{\partial^2[t(k)+U_0(\rho,k)]}{\partial k^2}\bigg|_{k_F} k_F^2 \\ &- \frac{1}{12}\frac{\partial^3[t(k)+U_0(\rho,k)]}{\partial k^3}\bigg|_{k_F} k_F^3 + \frac{5}{324}\frac{\partial^4[t(k)+U_0(\rho,k)]}{\partial k^4}\bigg|_{k_F} k_F^4 \\ &- \frac{10}{27}k_F\rho\frac{\partial}{\partial\rho}\frac{\partial[t(k)+U_0(\rho,k)]}{\partial k}\bigg|_{k_F} \\ &+ \frac{13}{54}k_F^2\rho\frac{\partial}{\partial\rho}\frac{\partial^2[t(k)+U_0(\rho,k)]}{\partial k^2}\bigg|_{k_F} \\ &- \frac{1}{18}k_F^3\rho\frac{\partial}{\partial\rho}\frac{\partial^3[t(k)+U_0(\rho,k)]}{\partial k^3}\bigg|_{k_F} \\ &+ \frac{1}{216}k_F^4\rho\frac{\partial}{\partial\rho}\frac{\partial^4[t(k)+U_0(\rho,k)]}{\partial k^4}\bigg|_{k_F} \\ &- \frac{11}{54}\frac{\partial U_{sym,1}(\rho,k)}{\partial k}\bigg|_{k_F} k_F - \frac{5}{36}\frac{\partial^2 U_{sym,1}(\rho,k)}{\partial k^2}\bigg|_{k_F} k_F^2 \\ &+ \frac{1}{6}\frac{\partial^3 U_{sym,1}(\rho,k)}{\partial k^3}\bigg|_{k_F} k_F^3 \\ &+ \frac{5}{9}k_F\rho\frac{\partial}{\partial\rho}\frac{\partial U_{sym,1}(\rho,k)}{\partial k}\bigg|_{k_F} - \frac{1}{3}k_F^2\rho\frac{\partial}{\partial\rho}\frac{\partial^2 U_{sym,1}(\rho,k)}{\partial k^2}\bigg|_{k_F} \\ &+ \frac{1}{18}k_F^3\rho\frac{\partial}{\partial\rho}\frac{\partial^3 U_{sym,1}(\rho,k)}{\partial k^3}\bigg|_{k_F}. \\ &+ \frac{13}{6}\frac{\partial U_{sym,2}(\rho,k)}{\partial k}\bigg|_{k_F} k_F + \frac{4}{3}\frac{\partial^2 U_{sym,2}(\rho,k)}{\partial k^2}\bigg|_{k_F} k_F^2 \\ &- k_F\rho\frac{\partial}{\partial\rho}\frac{\partial U_{sym,2}(\rho,k)}{\partial k}\bigg|_{k_F} + \frac{1}{2}k_F^2\rho\frac{\partial}{\partial\rho}\frac{\partial^2 U_{sym,2}(\rho,k)}{\partial k^2}\bigg|_{k_F} \\ &+ \frac{27}{2}U_{sym,3}(\rho,k_F) + 7\frac{\partial U_{sym,3}(\rho,k)}{\partial k}\bigg|_{k_F} k_F \\ &+ 3k_F\rho\frac{\partial}{\partial\rho}\frac{\partial U_{sym,3}(\rho,k)}{\partial k}\bigg|_{k_F} \\ &+ 18U_{sym,4}(\rho,k_F) + 9\rho\frac{\partial U_{sym,4}(\rho,k_F)}{\partial\rho}.\end{aligned} \tag{9c}$$

Similarly, taking the second derivative of Eq. (6) gives the skewness of $E_0(\rho)$ as follows:

$$\begin{aligned}J_0(\rho) = &27\rho^2\frac{\partial^2[t(k_F)+U_0(\rho,k_F)]}{\partial\rho^2} \\ &- 81\rho\frac{\partial[t(k_F)+U_0(\rho,k_F)]}{\partial\rho} \\ &+ 162[t(k_F)+U_0(\rho,k_F)] - 162E_0(\rho).\end{aligned} \tag{10}$$

2.3 The exact saturation density ρ_{sat} as a function of isospin asymmetry

For isospin asymmetric nuclear matter, the saturation density is different from that of the symmetric nuclear matter ρ_0. The former is defined as the exact saturation density and can be also written as a function of the isospin asymmetry δ [77]

$$\rho_{sat}(\delta) = \rho_0 + \rho_{sat,2}\delta^2 + \rho_{sat,4}\delta^4 + O(\delta^6). \tag{11}$$

For symmetric nuclear matter with $\delta = 0$, $\rho_{sat}(\delta)$ is reduced to ρ_0. According to the property of the saturation point $\frac{\partial E(\rho,\delta)}{\partial\rho}|_{\rho_{sat}(\delta)} = 0$ and expanding the EoS in terms of χ, the exact saturation density can be expressed as

$$\begin{aligned}\rho_{sat}(\delta) = &\rho_0 - \frac{3L_2(\rho_0)}{K_0(\rho_0)}\rho_0\cdot\delta^2 \\ &+ \left[\frac{3K_2(\rho_0)L_2(\rho_0)}{K_0(\rho_0)^2} - \frac{3L_4(\rho_0)}{K_0(\rho_0)} - \frac{3J_0(\rho_0)L_2^2(\rho_0)}{2K_0(\rho_0)^3}\right]\rho_0\cdot\delta^4.\end{aligned} \tag{12}$$

At the exact saturation density $\rho_{sat}(\delta)$, the energy per nucleon of asymmetric nuclear matter is given by

$$\begin{aligned}E_{sat}(\delta) &= E(\rho_{sat}(\delta),\delta) \\ &= E_0(\rho_0) + E_{sym,2}(\rho_0)\delta^2 + \left[E_{sym,4}(\rho_0) - \frac{L_2^2(\rho_0)}{2K_0(\rho_0)}\right]\delta^4 \\ &= E_{sat,0} + E_{sat,2}\delta^2 + E_{sat,4}\delta^4.\end{aligned} \tag{13}$$

The corresponding incompressibility coefficient of the EoS is

$$\begin{aligned}K_{sat}(\delta) &= 9\rho_{sat}^2(\delta)\frac{\partial^2 E(\rho,\delta)}{\partial^2\rho}|_{\rho_{sat}(\delta)} \\ &= K_0(\rho_0) + \left[K_2(\rho_0) - 6L_2(\rho_0) - \frac{J_0(\rho_0)}{K_0(\rho_0)}L_2(\rho_0)\right]\delta^2 + O(\delta^4) \\ &= K_{sat,0} + K_{sat,2}\delta^2 + O(\delta^4).\end{aligned} \tag{14}$$

It is clearly shown that the quartic symmetry energy at the exact saturation density is $E_{sat,4} = E_{sym,4}(\rho_0) - \frac{L_2^2(\rho_0)}{2K_0(\rho_0)}$, and the quadratic incompressibility coefficient is

$$K_{sat,2} = K_2(\rho_0) - 6L_2(\rho_0) - \frac{J_0(\rho_0)}{K_0(\rho_0)}L_2(\rho_0). \tag{15}$$

In previous studies [18, 29], $K_{sat,2}$ was approximated as $K_{sat,2} \to K_{asy,2} = K_2(\rho_0) - 6L_2(\rho_0)$ by neglecting the $-\frac{J_0(\rho_0)}{K_0(\rho_0)}L_2(\rho_0)$ term for simplicity. We will discuss its effect on $K_{sat,2}$ in the following section.

3 Results and discussions

We performed a systematic analysis of the basic quantities in the EoS of both symmetric and asymmetric nuclear matter at the saturation density ρ_0 by using 25 interaction parameter sets, which include two BGBD interactions with different neutron-proton effective masses [44–47], the MDI interaction with $x = -1$, 0, and 1 [47–50], 16 Skyrme interactions [62–72], and four Gogny interactions [73–75]. It is known that most of these interactions are fitted to the properties of finite nuclei, and the extrapolations to abnormal densities can be rather diverse. However, the comparison of a large number of results from different interactions could possibly provide useful information on the tendency of the density dependence of these basic quantities. Detailed numerical results from the total 25 interaction parameter sets are summarized in Table 1. The average values of the basic quantities in EoS are also given. For comparison, we also list the constraints summarized in other studies (see the last row of Table 1). As shown in Table 1, the calculated values of $E_0(\rho_0)$, $K_0(\rho_0)$, $E_{\mathrm{sym},2}(\rho_0)$, and $L_2(\rho_0)$ are consistent with the constraints extracted from both theoretical calculations and experimental data [18, 21, 25, 26]. Interestingly, the averaged $E_{\mathrm{sym},4}(\rho_0)$ value is almost the same as that in Ref. [77]. To further estimate the error bars of these basic quantities, all the calculated values in Table 1 are plotted in Figs. 2 and 3. It is seen from Fig. 2 that the data points of $E_0(\rho_0)$ and

Table 1 The saturation density ρ_0 (fm^{-3}) and basic quantities $E_0(\rho_0)$, $K_0(\rho_0)$, $J_0(\rho_0)$, $E_{\mathrm{sym},2}(\rho_0)$, $E_{\mathrm{sym},4}(\rho_0)$, $L_2(\rho_0)$, $L_4(\rho_0)$, $K_2(\rho_0)$, and $K_4(\rho_0)$ for totally 25 interaction sets in four kinds of interactions. The units of these quantities were MeV. In the last three rows, the averaged values and constraints in previous studies are shown. All interactions were taken from Ref. [44–50, 62–75]

Force	ρ_0	$E_0(\rho_0)$	$K_0(\rho_0)$	$J_0(\rho_0)$	$E_{\mathrm{sym},2}(\rho_0)$	$L_2(\rho_0)$	$K_2(\rho_0)$	$E_{\mathrm{sym},4}(\rho_0)$	$L_4(\rho_0)$	$K_4(\rho_0)$
BGBD										
Case-1	0.160	− 15.8	215.9	− 447.5	32.9	87.9	− 32.7	1.72	6.82	7.14
Case-2	0.160	− 15.8	215.9	− 447.5	33.0	121.8	101.0	− 0.73	− 4.26	7.14
MDI										
$x = 1$	0.160	− 16.1	212.4	− 447.3	30.5	14.7	− 264.0	0.62	0.53	− 4.83
$x = 0$	0.160	− 16.1	212.4	− 447.3	30.5	60.2	− 81.7	0.62	0.53	− 4.83
$x = -1$	0.160	− 16.1	212.4	− 447.3	30.5	105.8	100.6	0.62	0.53	− 4.83
Skyrme										
GSKI	0.159	− 16.0	230.3	− 405.7	32.0	63.5	− 95.3	0.38	0.56	− 1.61
GSKII	0.159	− 16.1	234.1	− 400.2	30.5	48.6	− 158.3	0.92	3.26	3.80
KDE0v1	0.165	− 16.2	228.4	− 386.3	34.6	54.7	− 127.4	0.46	0.92	− 0.94
LNS	0.175	− 15.3	211.5	− 384.0	33.5	61.5	− 127.7	0.82	2.67	2.44
MSL0	0.160	− 16.0	230.0	− 380.3	30.0	60.0	− 99.3	0.81	2.70	2.66
NRAPR	0.161	− 15.9	226.6	− 364.1	32.8	59.7	− 123.7	0.96	3.41	4.09
Ska25s20	0.161	− 16.1	221.5	− 415.0	34.2	65.1	− 118.2	0.46	0.93	0.88
Ska35s20	0.158	− 16.1	240.3	− 378.6	33.5	64.4	− 120.9	0.45	0.90	− 0.90
SKRA	0.159	− 15.8	216.1	− 377.2	31.3	53.0	− 138.8	0.95	3.39	4.07
SkT1	0.161	− 16.0	236.1	− 383.5	32.0	56.2	− 134.8	0.46	0.91	− 0.91
SkT2	0.161	− 15.9	235.7	− 382.6	32.0	56.2	− 134.7	0.46	0.91	− 0.91
SkT3	0.161	− 15.9	235.7	− 382.7	31.5	55.3	− 132.1	0.46	0.91	− 0.91
Skxs20	0.162	− 15.8	202.4	− 426.5	35.5	67.1	− 122.5	0.53	1.27	− 0.22
SQMC650	0.172	− 15.6	218.2	− 376.9	33.7	52.9	− 173.2	1.05	3.82	4.77
SQMC700	0.171	− 15.5	220.7	− 369.9	33.5	59.1	− 140.8	0.97	3.44	4.03
SV-sym32	0.159	− 15.9	232.8	− 378.3	31.9	57.0	− 148.2	0.89	3.11	3.50
Gogny										
D1	0.166	− 16.4	227.2	− 446.9	30.7	18.6	− 273.6	0.76	1.75	− 1.78
D1S	0.163	− 16.0	201.8	− 508.4	31.1	22.5	− 241.0	0.44	− 0.51	− 7.56
D1N	0.161	− 16.0	224.5	− 430.9	29.6	33.6	− 168.2	0.21	− 1.95	− 11.80
D1M	0.165	− 16.0	226.2	− 466.9	28.6	24.8	− 133.3	0.69	− 1.05	− 20.81
Average	0.162	− 15.94	222.8	− 411.3	32.0	57.0	− 123.6	0.64	1.42	− 1.25
Constraint		− 16	240		31.7	58.7		0.62		
Ref.		[18]	[21]		[25, 26]	[25, 26]		[77]		

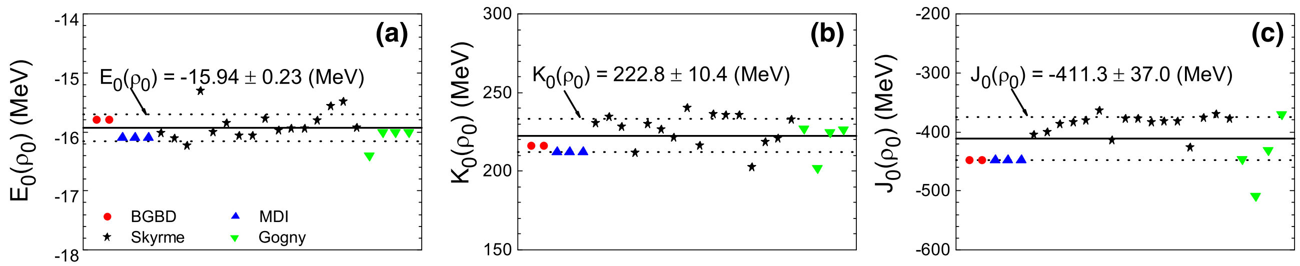

Fig. 2 (Color online) Values of basic quantities $E_0(\rho_0)$, $K_0(\rho_0)$, and $J_0(\rho_0)$ for symmetric nuclear matter at 25 parameter sets of the BGBD, MDI, Skyrme, and Gogny interactions. The solid and dashed lines represent the average values and their deviations, respectively

Fig. 3 (Color online) Values of $E_{\mathrm{sym},2}(\rho_0)$, $L_2(\rho_0)$, $K_2(\rho_0)$, $E_{\mathrm{sym},4}(\rho_0)$, $L_4(\rho_0)$, and $K_4(\rho_0)$ for asymmetric nuclear matter within 25 parameter sets of four kinds of interaction

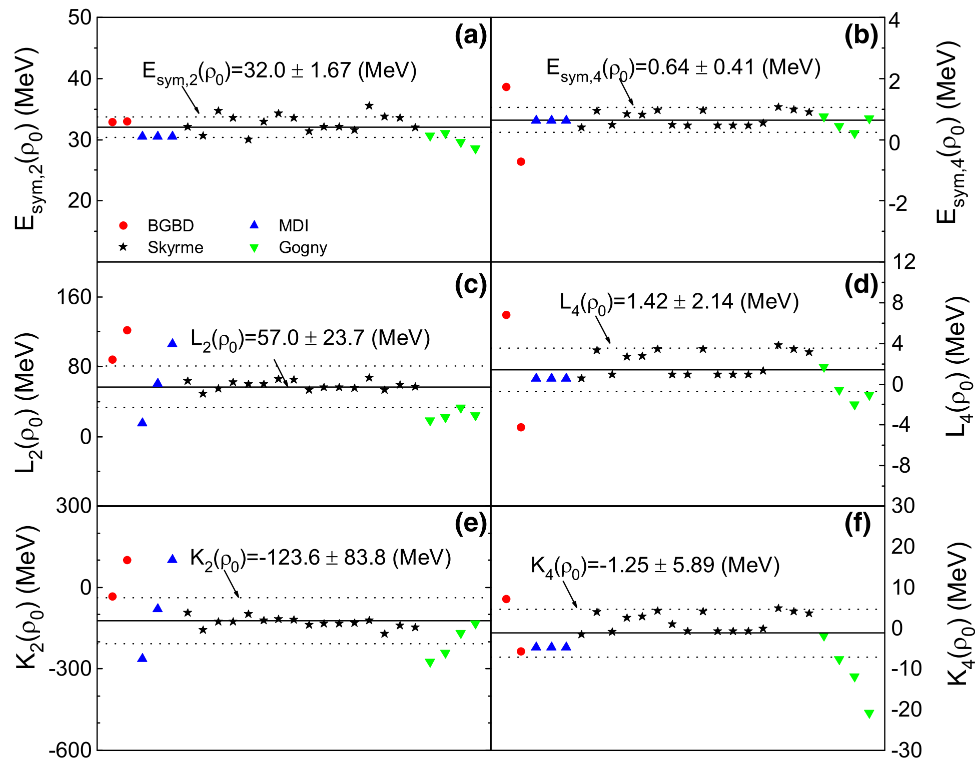

$K_0(\rho_0)$ are well constrained in a narrow range and the corresponding error bars are small. The error bar of skewness $J_0(\rho_0) = -411.3 \pm 37.0$ MeV is relatively large, especially for Gogny interactions. It is also noted that the skewness, together with $K_2(\rho_0)$, has recently received much attention in the calculation of the maximum mass of neutron stars and the radius of canonical neutron stars [15, 22, 23]. The error bars of the high-order terms $L_4(\rho_0)$, $K_2(\rho_0)$, and $K_4(\rho_0)$ are also given, that is, $L_4(\rho_0) = 1.42 \pm 2.14$ MeV, $K_2(\rho_0) = -123.6 \pm 83.8$ MeV, and $K_4(\rho_0) = -1.25 \pm 5.89$ MeV. In addition, for the MDI interaction, the $L_2(\rho_0)$ and $K_2(\rho_0)$ values with different spin(isospin)-dependent parameter x are scattered over a wide range. This is because the different choices of parameter x are to simulate very different density dependences of the symmetry energies at high densities [47–49].

In Fig. 4, we show the magnitudes of the separated terms $E_0(\rho)$, $E_{\mathrm{sym},2}(\rho)\delta^2$, $E_{\mathrm{sym},4}(\rho)\delta^4$ as well as the total one $E(\rho, \delta)$ at two different densities (ρ_0 and $2\rho_0$) and three different isospin asymmetries (δ^2=0.1, 0.2 and 0.5) by taking the NRAPR Skyrme interaction as an example. At the saturation density ρ_0 (see graphs (a)–(c)), the contribution of $E_0(\rho)$ to $E(\rho, \delta)$ is dominant. The contribution of $E_{\mathrm{sym},2}(\rho)\delta^2$ increases with an increase in isospin asymmetry δ. It is also shown that the contribution from $E_{\mathrm{sym},4}(\rho)\delta^4$ is small and comes into play at large isospin asymmetry with $\delta^2 = 0.5$. At $2\rho_0$ (see graphs (d)–(f)), the $E_0(\rho)$ contribution is suppressed compared with that at ρ_0, while $E_{\mathrm{sym},2}(\rho)\delta^2$ plays a more important role in the EoS, especially at $\delta^2 = 0.5$. It should also be noted that $E_{\mathrm{sym},4}(\rho)$ contributes only at a very high density and large isospin asymmetry. The magnitude of $E_{\mathrm{sym},4}(\rho)$ can

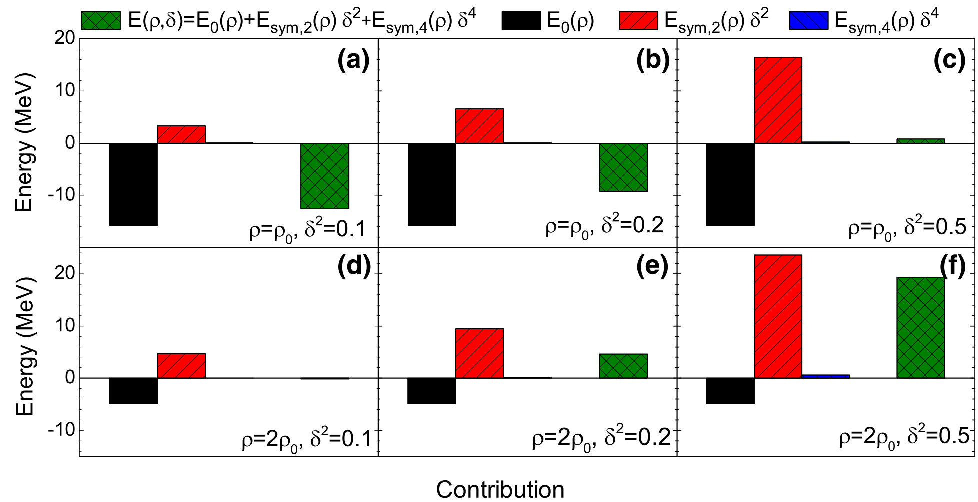

Fig. 4 (Color online) The magnitudes of $E_0(\rho)$, $E_{\mathrm{sym},2}(\rho)\delta^2$, and $E_{\mathrm{sym},4}(\rho)\delta^4$ in the EoS at two different ρ values and three different δ^2 values. The NRAPR Skyrme interaction is applied

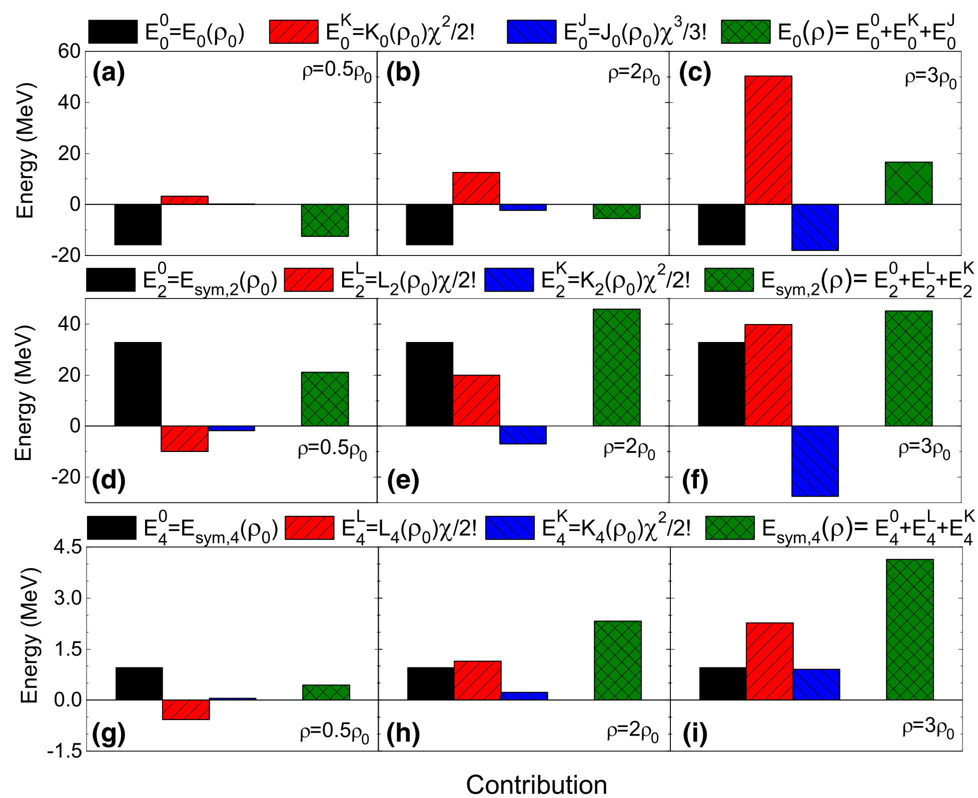

Fig. 5 (Color online) The magnitude of each order in $E_0(\rho)$, $E_{\mathrm{sym},2}(\rho)$ and $E_{\mathrm{sym},4}(\rho)$ expressed by $E_0(\rho_0)$, $K_0(\rho_0)$ and $J_0(\rho_0)$, $E_{\mathrm{sym},2}(\rho_0)$, $L_2(\rho_0)$ and $K_2(\rho_0)$, and $E_{\mathrm{sym},4}(\rho_0)$, $L_4(\rho_0)$ and $K_4(\rho_0)$, respectively. The NRAPR Skyrme interaction was applied

significantly affect the calculation of the proton fraction in neutron stars at β-equilibrium [14, 41].

We further expand $E_0(\rho)$, $E_{\mathrm{sym},2}(\rho)$, and $E_{\mathrm{sym},4}(\rho)$ as a series of χ with their corresponding slopes and incompressibility coefficients. In Fig. 5, we depict the contributions from each term at different densities $0.5\rho_0$, $2\rho_0$ and $3\rho_0$. As can be observed in Fig. 5, the first-order terms E_0^0 ($E_0(\rho_0)$), E_2^0 ($E_{\mathrm{sym},2}(\rho_0)$), and E_4^0 ($E_{\mathrm{sym},4}(\rho_0)$) contribute largely at all densities. E_0^{K} and E_0^{J} terms become increasingly important with increasing density. For $E_{\mathrm{sym},2}(\rho)$ and $E_{\mathrm{sym},4}(\rho)$ at $3\rho_0$, the contributions from the slopes (E_2^{L} and E_4^{L}) and the incompressibility coefficients (E_2^{K} and E_4^{K}) are much larger than those at $0.5\rho_0$ and $2\rho_0$. In particular, the E_0^{J}, E_2^{K}, and E_4^{K} terms at $3\rho_0$ can be as important as the first-order terms. Thus, high-order terms should be considered when analyzing the properties of nuclear matter systems at high densities, such as neutron stars.

More interestingly, the basic quantities at the saturation density are decomposed into the kinetic energy $t(k)$ and the symmetric and asymmetric parts of the single-nucleon potential $U_0(\rho,k)$ and $U_{\mathrm{sym,i}}(\rho,k)$. As shown in Fig. 6, the

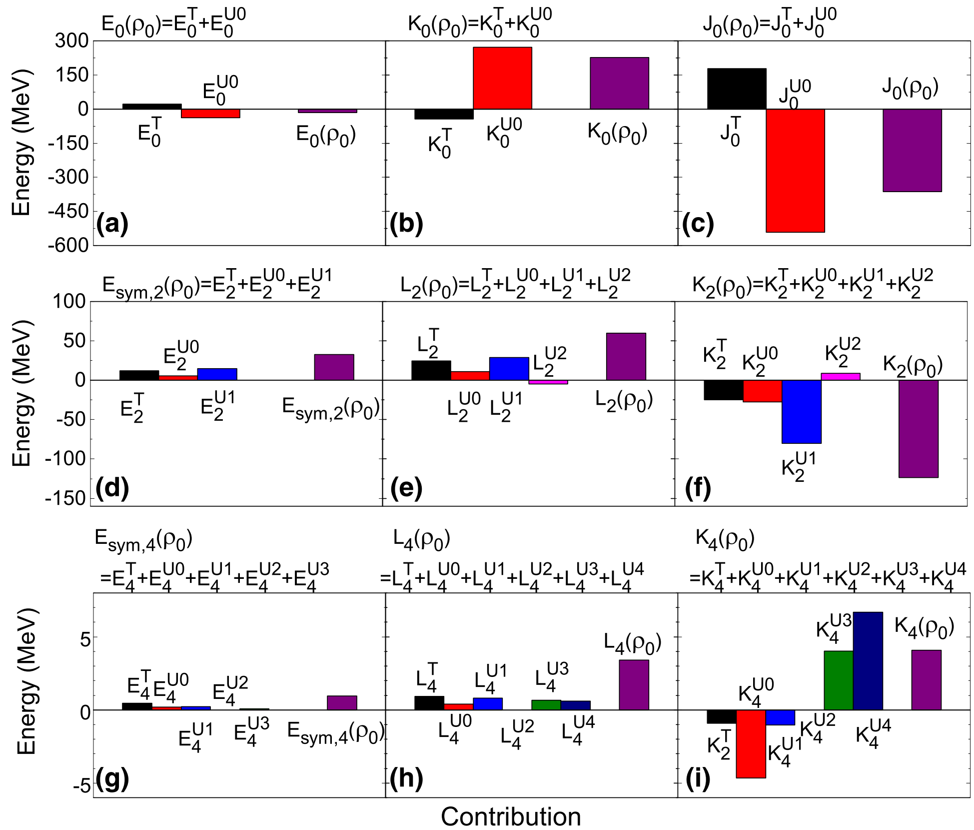

Fig. 6 (Color online) The single-nucleon potential decomposition of $E_0(\rho_0)$, $K_0(\rho_0)$, $J_0(\rho_0)$, $E_{\rm sym,2}(\rho_0)$, $L_2(\rho_0)$, $K_2(\rho_0)$, $E_{\rm sym,4}(\rho_0)$, $L_4(\rho_0)$, and $K_4(\rho_0)$. The NRAPR Skyrme interaction is applied

contributions from different terms $t(k)$, $U_0(\rho,k)$ and $U_{\rm sym,i}(\rho,k)(i=1,2,3,4)$ are denoted by superscripts of T, $U0$, $U1$, $U2$, $U3$ and $U4$, respectively. It is clear that $E_0(\rho_0)$, $K_0(\rho_0)$, and $J_0(\rho_0)$ are completely determined by $t(k)$ and $U_0(\rho,k)$. For other quantities, the contributions from the asymmetric parts $U_{\rm sym,1}(\rho,k)$, $U_{\rm sym,2}(\rho,k)$, $U_{\rm sym,3}(\rho,k)$, and $U_{\rm sym,4}(\rho,k)$ cannot be neglected. It is clearly shown that the first-order term $U_{\rm sym,1}(\rho,k)$ contributes to all six basic quantities. The second-order term $U_{\rm sym,2}(\rho,k)$ does not contribute to $E_{\rm sym,2}(\rho_0)$, but to its corresponding slope $L_2(\rho_0)$ and the incompressibility coefficient $K_2(\rho_0)$. In principle, the $U_{\rm sym,2}(\rho,k)$ term should also contribute to the fourth-order terms $E_{\rm sym,4}(\rho_0)$, $L_4(\rho_0)$, and $K_4(\rho_0)$, but for the Skyrme interaction, $U_{\rm sym,2}(\rho,k)$ is not momentum-dependent and does not contribute. In addition, there are very few studies on the contributions of high-order terms $U_{\rm sym,3}(\rho,k)$ and $U_{\rm sym,4}(\rho,k)$ to the basic quantities. In Fig. 7, we show the density-dependence of $U_0(\rho,k_{\rm F})$, $U_{\rm sym,1}(\rho,k_{\rm F})$, $U_{\rm sym,2}(\rho,k_{\rm F})$, $U_{\rm sym,3}(\rho,k_{\rm F})$ and $U_{\rm sym,4}(\rho,k_{\rm F})$ at the Fermi momentum $k_{\rm F}=(3\pi^2\rho/2)^{1/3}$ by using the NRAPR Skyrme interaction. It can be clearly seen in Fig. 7 that the magnitudes of $U_0(\rho,k_{\rm F})$ and $U_{\rm sym,1}(\rho,k_{\rm F})$ are generally very large, while the ones of $U_{\rm sym,2}(\rho,k_{\rm F})$, $U_{\rm sym,3}(\rho,k_{\rm F})$ and $U_{\rm sym,4}(\rho,k_{\rm F})$ are very small but increase with the

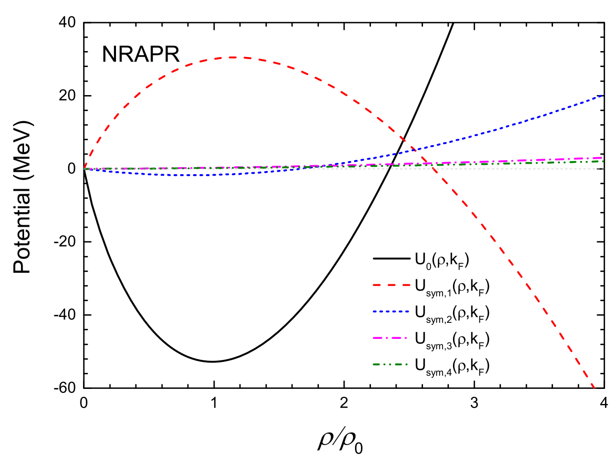

Fig. 7 (Color online) The density-dependence of $U_0(\rho,k_{\rm F})$, $U_{sym,1}(\rho,k_{\rm F})$, $U_{\rm sym,2}(\rho,k_{\rm F})$, $U_{\rm sym,3}(\rho,k_{\rm F})$, and $U_{\rm sym,4}(\rho,k_{\rm F})$. The NRAPR Skyrme interaction was applied

increasing density. Our results indicate that the $U_{\rm sym,3}(\rho,k)$ and $U_{\rm sym,4}(\rho,k)$ contributions should be taken into account for the fourth-order terms to understand the properties of asymmetric nuclear matter, especially for the cases with very large isospin asymmetries and high densities.

By analyzing the isospin dependence of the saturation properties of asymmetric nuclear matter, a number of

Table 2 The calculated values of expansion coefficients ρ_0 (fm^{-3}), $\rho_{\mathrm{sat},2}$ (fm^{-3}), $\rho_{\mathrm{sat},4}$ (fm^{-3}), the quartic symmetry energy $E_{\mathrm{sat},4}$ (MeV), the quadratic incompressibility coefficient $K_{\mathrm{sat},2}$ (MeV), and its two main components $K_{\mathrm{asy},2}$ (MeV) and $J_0(\rho_0)/K_0(\rho_0)$. In the last three rows, the averaged values and constraints in previous studies are shown

Force	ρ_0	$\rho_{\mathrm{sat},2}$	$\rho_{\mathrm{sat},4}$	$E_{\mathrm{sat},4}$	$K_{\mathrm{asy},2}$	$K_{\mathrm{sat},2}$	$J_0(\rho_0)/K_0(\rho_0)$
BGBD							
Case-1	0.160	− 0.195	0.038	− 16.17	− 560.1	− 377.9	− 2.07
Case-2	0.160	− 0.271	0.295	− 35.11	− 630.0	− 377.5	− 2.07
MDI							
$x = 1$	0.160	− 0.033	− 0.040	0.11	− 352.2	− 321.2	− 2.11
$x = 0$	0.160	− 0.136	− 0.013	− 7.91	− 442.9	− 316.1	− 2.11
$x = -1$	0.160	− 0.239	0.237	− 25.73	− 534.2	− 311.4	− 2.11
Skyrme							
GSKI	0.159	− 0.131	− 0.024	− 8.36	− 476.03	− 364.23	− 1.76
GSKII	0.159	− 0.099	− 0.056	− 4.12	− 450.04	− 366.94	− 1.71
KDE0v1	0.165	− 0.119	− 0.044	− 6.09	− 455.71	− 363.13	− 1.69
LNS	0.175	− 0.153	− 0.059	− 8.12	− 496.75	− 385.10	− 1.82
MSL0	0.160	− 0.125	− 0.033	− 7.01	− 459.33	− 360.11	− 1.65
NRAPR	0.161	− 0.127	− 0.050	− 6.90	− 481.82	− 385.91	− 1.61
Ska25s20	0.161	− 0.142	− 0.039	− 9.11	− 508.89	− 386.89	− 1.87
Ska35s20	0.158	− 0.127	− 0.039	− 8.19	− 507.47	− 405.95	− 1.58
SKRA	0.159	− 0.117	− 0.058	− 5.55	− 456.89	− 364.36	− 1.75
SkT1	0.161	− 0.115	− 0.045	− 6.23	− 471.90	− 380.66	− 1.62
SkT2	0.161	− 0.115	− 0.045	− 6.23	− 471.62	− 380.45	− 1.62
SkT3	0.161	− 0.113	− 0.044	− 6.03	− 463.93	− 374.14	− 1.62
Skxs20	0.162	− 0.161	− 0.044	− 10.60	− 525.16	− 383.74	− 2.11
SQMC650	0.172	− 0.125	− 0.082	− 5.37	− 490.78	− 399.34	− 1.73
SQMC700	0.171	− 0.137	− 0.065	− 6.93	− 495.14	− 396.16	− 1.68
SV-sym32	0.159	− 0.117	− 0.057	− 6.10	− 490.44	− 397.74	− 1.62
Gogny							
D1	0.166	− 0.041	− 0.050	0.001	− 385.2	− 348.6	− 1.97
D1S	0.163	− 0.055	− 0.056	− 0.81	− 376.0	− 319.3	− 2.52
D1N	0.161	− 0.072	− 0.039	− 2.30	− 369.8	− 305.3	− 1.92
D1M	0.165	− 0.054	− 0.023	− 0.67	− 282.1	− 230.9	− 2.06
Average	0.162	− 0.125	− 0.017	− 7.98	− 465.4	− 360.1	− 1.86
Constraint					− 500	− 370/− 550	
Ref.					[31]	[77] [27, 28]	

important quantities are calculated using 25 interaction parameter sets, and their numerical results as well as their averaged values are also listed in Table 2. For comparison, the constraints of $K_{\mathrm{asy},2}$ and $K_{\mathrm{sat},2}$ from other studies are listed in the last row of Table 2. It is shown that the second-order coefficient $\rho_{\mathrm{sat},2}$, one of the most important isospin-dependent parts of $\rho_{\mathrm{sat}}(\delta)$, has a negative value in all cases, and the fourth-order coefficient $\rho_{\mathrm{sat},4}$ also has a negative value for the Skyrme and Gogny interactions. This means that in most cases, the saturation density of asymmetric nuclear matter is lower than that of symmetric nuclear matter, especially at larger isospin asymmetry δ (see graph (a) of Fig. 8). For the BGBD interaction (Case-2), the calculated value of $\rho_{\mathrm{sat},4}$ is positive and relatively large. According to the relationship in Eq. (11), this would lead to a higher saturation density of asymmetric nuclear matter than that of symmetric nuclear matter with isospin asymmetry δ close to unity. For asymmetric nuclear matter at $\rho_{\mathrm{sat}}(\delta)$, the corresponding $E_{\mathrm{sat},4}$ values are rather diverse and are considered to be important for the proton fraction in neutron stars.

As shown in graph (b) of Fig. 8, the results of $K_2(\rho_0)$, $K_{\mathrm{asy},2}$, and $K_{\mathrm{sat},2}$ are given and their values are constrained to be $K_2 = -123.6 \pm 83.8$ MeV, $K_{\mathrm{asy},2} = -465.4 \pm 70.0$ MeV, and $K_{\mathrm{sat},2} = -360.1 \pm 39.0$ MeV, respectively. The averaged $K_{\mathrm{asy},2}$ value is close to the previous theoretical constraint of -500 ± 50 MeV given in Ref. [31] if the error bar is considered. In Table 2, there are two previous constraints for $K_{\mathrm{sat},2}$. One is $K_{\mathrm{sat},2} = -370 \pm 120$ MeV from a modified Skyrme-like (MSL) model [77], and the other is

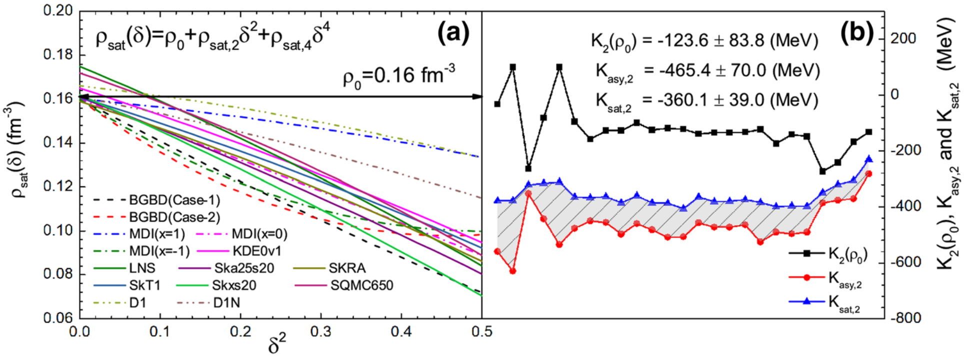

Fig. 8 (Color online) The isospin-dependence of the exact saturation density $\rho_{sat}(\delta)$ within 14 typical interaction parameter sets in graph (**a**) and the comparisons between the error bars of the quadratic incompressibility coefficients $K_2(\rho_0)$, $K_{asy,2}$, and $K_{sat,2}$ calculated by using 25 interaction parameter sets in graph (**b**)

-550 ± 100 MeV by analyzing the measured data of the isotopic dependence of the giant monopole resonance (GMR) in the even-A Sn isotopes [27, 28]. Compared with these previous studies, it is clear that the $K_{asy,2}$ and $K_{sat,2}$ values remain uncertain and require more data to further constrain their values. In addition, as mentioned before, the term $-\frac{J_0(\rho_0)}{K_0(\rho_0)}L_2(\rho_0)$ in Eq. (15) is typically ignored for simplicity. However, this is clearly shown in Fig. 8b that the contribution of this term is non-negligible. In the present work, we include the contribution of this high-order term, and the ratio $J_0(\rho_0)/K_0(\rho_0)$ is constrained in the range of -1.86 ± 0.23. Finally, we obtain a simple relation for $K_{sat,2}$

$$K_{sat,2} = K_2(\rho_0) - 4.14L_2(\rho_0). \tag{16}$$

With the averaged results $L_2(\rho_0) = 57.0$ MeV and $K_2(\rho_0) = -123.6$ MeV, the calculated value $K_{sat,2} = -359.6$ MeV is in good agreement with the average value of -360.1 ± 39.0 MeV from the 25 interaction sets. This simple empirical relation could be useful for estimating the value of $K_{sat,2}$ for asymmetric nuclear matter.

4 Summary

Based on the Hugenholtz–Van Hove theorem, the general expressions for the six basic quantities of EoS are expanded in terms of the kinetic energy $t(k)$, the symmetric and asymmetric parts of the global optical potential $U_0(\rho,k)$ and $U_{sym,i}(\rho,k)$. The analytical expressions of the coefficients $K_2(\rho)$ and $K_4(\rho)$ are given for the first time. By using 25 types of interaction sets, the values of these quantities were systematically calculated at the saturation density ρ_0. It is emphasized that there are very few studies on quantities $L_4(\rho_0)$, $K_2(\rho_0)$, and $K_4(\rho_0)$ and their average values from a total of 25 interaction sets are $L_4(\rho_0) = 1.42 \pm 2.14$ MeV, $K_2(\rho_0) = -123.6 \pm 83.8$ MeV, and $K_4(\rho_0) = -1.25 \pm 5.89$ MeV, respectively. The averaged values of the other quantities were consistent with those of previous studies. Furthermore, the different contributions of the kinetic term, the isoscalar and isovector potentials to these basic quantities were systematically analyzed at saturation density. It is clearly shown that $t(k_F)$ and $U_0(\rho,k_F)$ play vital roles in determining the EoS of both symmetric and asymmetric nuclear matter. For asymmetric nuclear matter, $U_{sym,1}(\rho,k)$ contributes to all the quantities, whereas $U_{sym,2}(\rho,k)$ does not contribute to $E_{sym,2}(\rho_0)$, but contributes to the second-order terms $L_2(\rho_0)$ and $K_2(\rho_0)$ as well as the fourth-order terms $E_{sym,4}(\rho_0)$, $L_4(\rho_0)$, and $K_4(\rho_0)$. In addition, the contribution from $U_{sym,3}(\rho,k)$ cannot be neglected for $E_{sym,4}(\rho_0)$, $L_4(\rho_0)$, and $K_4(\rho_0)$. $U_{sym,4}(\rho,k)$ should also be included in the calculations for $L_4(\rho_0)$ and $K_4(\rho_0)$. In addition, the quadratic incompressibility coefficient at $\rho_{sat}(\delta)$ is found to have a simple empirical relation $K_{sat,2} = K_2(\rho_0) - 4.14L_2(\rho_0)$ based on the present analysis.

Author Contributions All authors contributed to the study conception and design. Material preparation, data collection and analysis were performed by Jie Liu, Chao Gao, Niu Wan and Chang Xu. The first draft of the manuscript was written by Jie Liu and all authors commented on previous versions of the manuscript. All authors read and approved the final manuscript.

References

1. P. Danielewicz, R. Lacey, W.G. Lynch, Determination of the equation of state of dense matter. Science **298**, 1592 (2002). https://doi.org/10.1126/science.1078070
2. J.M. Lattimer, M. Prakash, The physics of neutron stars. Science **304**, 536 (2004). https://doi.org/10.1126/science.1090720
3. M. Baldo, G.F. Burgio, The nuclear symmetry energy. Prog. Part. Nucl. Phys. **91**, 203 (2016). https://doi.org/10.1016/j.ppnp.2016.06.006
4. C.J. Jiang, Y. Qiang, D.W. Guan et al., From finite nuclei to neutron stars: the essential role of high-order density dependence in effective forces. Chin. Phys. Lett. **38**, 052101 (2021). https://doi.org/10.1088/0256-307X/38/5/052101
5. X.L. Ren, C.X. Chen, K.W. Li et al., Relativistic chiral description of the $^1S_0$ nucleon-nucleon scattering. Chin. Phys.

Lett. **38**, 062101 (2021). https://doi.org/10.1088/0256-307X/38/6/062101
6. M. Bender, P.H. Heenen, P.G. Reinhard, Self-consistent mean-field models for nuclear structure. Rev. Mod. Phys. **75**, 121 (2003). https://doi.org/10.1103/RevModPhys.75.121
7. J. Xu, Constraining isovector nuclear interactions with giant dipole resonance and neutron skin in ^{208}Pb from a Bayesian approach. Chin. Phys. Lett. **38**, 042101 (2021). https://doi.org/10.1088/0256-307X/38/4/042101
8. H. Yu, D.Q. Fang, Y.G. Ma, Investigation of the symmetry energy of nuclear matter using isospin-dependent quantum molecular dynamics. Nucl. Sci. Tech. **31**, 61 (2020). https://doi.org/10.1007/s41365-020-00766-x
9. J.M. Dong, W. Zuo, J.Z. Gu, Origin of symmetry energy in finite nuclei and density dependence of nuclear matter symmetry energy from measured α-decay energies. Phys. Rev. C **87**, 014303 (2013). https://doi.org/10.1103/PhysRevC.87.014303
10. L.W. Chen, C.M. Ko, B.A. Li et al., Probing isospin- and momentum-dependent nuclear effective interactions in neutron-rich matter. Eur. Phys. J. A **50**, 29 (2014). https://doi.org/10.1140/epja/i2014-14029-6
11. O. Li, Z.X. Li, X.Z. Wu et al., Disentangling the effects of thickness of the neutron skin and symmetry potential in nucleon induced reactions on Sn isotopes. Chin. Phys. Lett. **26**, 052501 (2009). https://doi.org/10.1088/0256-307X/26/5/052501
12. G.F. Wei, Q.J. Zhi, X.W. Cao et al., Examination of an isospin-dependent single-nucleon momentum distribution for isospin-asymmetric nuclear matter in heavy-ion collisions. Nucl. Sci. Tech. **31**, 71 (2020). https://doi.org/10.1007/s41365-020-00779-6
13. G. Coló, U. Garg, H. Sagawa, Symmetry energy from the nuclear collective motion: constraints from dipole, quadrupole, monopole and spin-dipole resonances. Eur. Phys. J. A **50**, 26 (2014). https://doi.org/10.1140/epja/i2014-14026-9
14. J. Xu, L.W. Chen, B.A. Li et al., Locating the inner edge of the neutron star crust using terrestrial nuclear laboratory data. Phys. Rev. C **79**, 035802 (2009). https://doi.org/10.1103/PhysRevC.79.035802
15. B.A. Li, P.G. Krastev, D.H. Wen et al., Towards understanding astrophysical effects of nuclear symmetry energy. Eur. Phys. J. A **55**, 23 (2019). https://doi.org/10.1140/epja/i2019-12780-8
16. Y. Xu, Q.J. Zhi, Y.B. Wang et al., Nucleonic $^1S_0$ superfluidity induced by a soft pion in neutron star matter with antikaon condensations. Chin. Phys. Lett. **36**, 061301 (2019). https://doi.org/10.1088/0256-307X/36/6/061301
17. B.A. Li, N.B. Zhang, Astrophysical constraints on a parametric equation of state for neutron-rich nucleonic matter. Nucl. Sci. Tech. **29**, 178 (2018). https://doi.org/10.1007/s41365-018-0515-9
18. B.A. Li, L.W. Chen, C.M. Ko, Recent progress and new challenges in isospin physics with heavy-ion reactions. Phys. Rep. **464**, 113 (2008). https://doi.org/10.1016/j.physrep.2008.04.005
19. J.P. Blaizot, Nuclear compressibilities. Phys. Rep. **64**, 171 (1980). https://doi.org/10.1016/0370-1573(80)90001-0
20. D.H. Youngblood, H.L. Clark, Y.W. Lui, Incompressibility of nuclear matter from the giant monopole resonance. Phys. Rev. Lett. **82**, 691 (1999). https://doi.org/10.1103/PhysRevLett.82.691
21. S. Shlomo, V.M. Kolomietz, G. Colò, Deducing the nuclear-matter incompressibility coefficient from data on isoscalar compression modes. Eur. Phys. J. A **30**, 23 (2006). https://doi.org/10.1140/epja/i2006-10100-3
22. N.B. Zhang, B.A. Li, J. Xu, Combined constraints on the equation of state of dense neutron-rich matter from terrestrial nuclear experiments and observations of neutron stars. Astrophys. J. **859**, 90 (2018). https://doi.org/10.3847/1538-4357/aac027
23. W.J. Xie, B.A. Li, Bayesian inference of high-density nuclear symmetry energy from radii of canonical neutron stars. Astrophys. J. **883**, 174 (2019). https://doi.org/10.3847/1538-4357/ab3f37
24. B.J. Cai, L.W. Chen, Constraints on the skewness coefficient of symmetric nuclear matter within the nonlinear relativistic mean field model. Nucl. Sci. Tech. **28**, 185 (2017). https://doi.org/10.1007/s41365-017-0329-1
25. B.A. Li, H. Xiao, Constraining the neutron-proton effective mass splitting using empirical constraints on the density dependence of nuclear symmetry energy around normal density. Phys. Lett. B **727**, 276 (2013). https://doi.org/10.1016/j.physletb.2013.10.006
26. M. Oertel, M. Hempel, T. Klähn et al., Equations of state for supernovae and compact stars. Rev. Mod. Phys. **89**, 015007 (2017). https://doi.org/10.1103/RevModPhys.89.015007
27. U. Garg, T. Li, S. Okumura et al., The giant monopole resonance in the Sn isotopes: why is Tin so fluffy? Nucl. Phys. A **788**, 36–43 (2007). https://doi.org/10.1016/j.nuclphysa.2007.01.046
28. T. Li, U. Garg, Y. Liu et al., Isotopic dependence of the giant monopole resonance in the even-A $^{112-124}Sn$ isotopes and the asymmetry term in nuclear incompressibility. Phys. Rev. Lett. **99**, 162503 (2007). https://doi.org/10.1103/PhysRevLett.99.162503
29. M. Lopez-Quelle, S. Marcos, R. Niembro et al., Asymmetric nuclear matter in the relativistic approach. Nucl. Phys. A **483**, 479 (1988). https://doi.org/10.1016/0375-9474(88)90080-2
30. Z.G. Xiao, B.A. Li, L.W. Chen et al., Circumstantial evidence for a soft nuclear symmetry energy at suprasaturation densities. Phys. Rev. Lett. **102**, 062502 (2009). https://doi.org/10.1103/PhysRevLett.102.062502
31. L.W. Chen, C.M. Ko, B.A. Li, Isospin-dependent properties of asymmetric nuclear matter in relativistic mean field models. Phys. Rev. C **76**, 054316 (2007). https://doi.org/10.1103/PhysRevC.76.054316
32. C. Xu, Z.Z. Ren, Effect of short-range and tensor force correlations on high-density behavior of symmetry energy. Chin. Phys. Lett. **29**, 122102 (2012). https://doi.org/10.1088/0256-307X/29/12/122102
33. N.B. Zhang, B.J. Cai, B.A. Li et al., How tightly is the nuclear symmetry energy constrained by a unitary Fermi gas? Nucl. Sci. Tech. **28**, 181 (2017). https://doi.org/10.1007/s41365-017-0336-2
34. J. Pu, Z. Zhang, L.W. Chen, Nuclear matter fourth-order symmetry energy in nonrelativistic mean-field models. Phys. Rev. C **96**, 054311 (2017). https://doi.org/10.1103/PhysRevC.96.054311
35. Z.W. Liu, Z. Qian, R.Y. Xing et al., Nuclear fourth-order symmetry energy and its effects on neutron star properties in the relativistic Hartree–Fock theory. Phys. Rev. C **97**, 025801 (2018). https://doi.org/10.1103/PhysRevC.97.025801
36. J.M. Dong, W. Zuo, J.Z. Gu, The fourth-order symmetry energy of finite nuclei. Phys. Atom. Nucl. **81**, 283 (2018). https://doi.org/10.1134/S1063778818030109
37. C.G. Boquera, M. Centelles, X. Viñas et al., Higher-order symmetry energy and neutron star core-crust transition with Gogny forces. Phys. Rev. C **96**, 065806 (2017). https://doi.org/10.1103/PhysRevC.96.065806
38. N.M. Hugenholtz, L. Van Hove, A theorem on the single particle energy in a Fermi gas with interaction. Physica **24**, 363 (1958). https://doi.org/10.1016/S0031-8914(58)95281-9
39. N. Wan, C. Xu, Z.Z. Ren, α-Decay half-life screened by electrons. Nucl. Sci. Tech. **27**, 149 (2016). https://doi.org/10.1007/s41365-016-0150-2
40. N. Wan, C. Xu, Z.Z. Ren et al., Constraints on both the symmetry energy $E_2(\rho_0)$ and its density slope $L_2(\rho_0)$ by cluster radioactivity. Phys. Rev. C **96**, 044331 (2017). https://doi.org/10.1103/PhysRevC.96.044331
41. C. Xu, B.A. Li, L.W. Chen et al., Analytical relations between nuclear symmetry energy and single-nucleon potentials in isospin asymmetric nuclear matter. Nucl. Phys. A **865**, 1 (2011). https://doi.org/10.1016/j.nuclphysa.2011.06.027

42. C. Xu, B.A. Li, L.W. Chen, Attempt to link the neutron skin thickness of ^{208}Pb with the symmetry energy through cluster radioactivity. Phys. Rev. C **90**, 064310 (2014). https://doi.org/10.1103/PhysRevC.90.064310
43. M. Ji, C. Xu, Quantum anti-Zeno effect in nuclear β decay. Chin. Phys. Lett. **38**, 032301 (2021). https://doi.org/10.1088/0256-307X/38/3/032301
44. C. Gale, G. Bertsch, S. Das Gupta, Heavy-ion collision theory with momentum-dependent interactions. Phys. Rev. C **35**, 1666 (1987). https://doi.org/10.1103/PhysRevC.35.1666
45. I. Bombaci, U. Lombardo, Asymmetric nuclear matter equation of state. Phys. Rev. C **44**, 1892 (1991). https://doi.org/10.1103/PhysRevC.44.1892
46. J. Rizzo, M. Colonna, M. Di Toro et al., Transport properties of isospin effective mass splitting. Nucl. Phys. A **732**, 202 (2004). https://doi.org/10.1016/j.nuclphysa.2003.11.057
47. C.B. Das, S. Das Gupta, C. Gale et al., Momentum dependence of symmetry potential in asymmetric nuclear matter for transport model calculations. Phys. Rev. C **67**, 034611 (2003). https://doi.org/10.1103/PhysRevC.67.034611
48. B.A. Li, C.B. Das, S. Das Gupta et al., Effects of momentum-dependent symmetry potential on heavy-ion collisions induced by neutron-rich nuclei. Nucl. Phys. A **735**, 563 (2004). https://doi.org/10.1016/j.nuclphysa.2004.02.016
49. B.A. Li, C.B. Das, S. Das Gupta et al., Momentum dependence of the symmetry potential and nuclear reactions induced by neutron-rich nuclei at RIA. Phys. Rev. C **69**, 011603(R) (2004). https://doi.org/10.1103/PhysRevC.69.011603
50. L.W. Chen, C.M. Ko, B.A. Li, Determination of the stiffness of the nuclear symmetry energy from isospin diffusion. Phys. Rev. Lett. **94**, 032701 (2005). https://doi.org/10.1103/PhysRevLett.94.032701
51. Z.Q. Feng, Momentum dependence of the symmetry potential and its influence on nuclear reactions. Phys. Rev. C **84**, 024610 (2011). https://doi.org/10.1103/PhysRevC.84.024610
52. Z.Q. Feng, Nuclear in-medium effects and collective flows in heavy-ion collisions at intermediate energies. Phys. Rev. C **85**, 014604 (2012). https://doi.org/10.1103/PhysRevC.85.014604
53. F. Zhang, J. Su, Probing neutron-proton effective mass splitting using nuclear stopping and isospin mix in heavy-ion collisions in GeV energy region. Nucl. Sci. Tech. **31**, 77 (2020). https://doi.org/10.1007/s41365-020-00787-6
54. T.H.R. Skyrme, The effective nuclear potential. Nucl. Phys. **9**, 615 (1959). https://doi.org/10.1016/0029-5582(58)90345-6
55. Y.Z. Wang, Y. Li, C. Qi et al., Pairing effects on bubble nuclei. Chin. Phys. Lett. **36**, 032101 (2019). https://doi.org/10.1088/0256-307X/36/3/032101
56. D. Vautherin, D.M. Brink, Hartree–Fock calculations with Skyrme's interaction. I. Spherical nuclei. Phys. Rev. C **5**, 626 (2012). https://doi.org/10.1103/PhysRevC.5.626
57. D.M. Brink, E. Boeker, Effective interactions for Hartree–Fock calculations. Nucl. Phys. A **91**, 1 (1967). https://doi.org/10.1016/0375-9474(67)90446-0
58. D. Gogny, R. Padjen, The propagation and damping of the collective modes in nuclear matter. Nucl. Phys. A **293**, 365 (1977). https://doi.org/10.1016/0375-9474(77)90104-X
59. J. Dechargé, M. Girod, D. Gogny, Self consistent calculations and quadrupole moments of even Sm isotopes. Phys. Lett. B **55**, 361 (1975). https://doi.org/10.1016/0370-2693(75)90359-7
60. J. Boguta, A.R. Bodmoer, Relativistic calculation of nuclear matter and the nuclear surface. Nucl. Phys. A **292**, 413 (1977). https://doi.org/10.1016/0375-9474(77)90626-1
61. F. Ouyang, B.B. Liu, W. Chen, Nuclear symmetry energy from a relativistic mean field theory. Chin. Phys. Lett. **30**, 092101 (2013). https://doi.org/10.1088/0256-307X/30/9/092101
62. M. Dutra, O. Lourenço, J.S. Sá Martins et al., Skyrme interaction and nuclear matter constraints. Phys. Rev. C **85**, 035201 (2012). https://doi.org/10.1103/PhysRevC.85.035201
63. A.W. Steiner, M. Prakash, J.M. Lattimer et al., Isospin asymmetry in nuclei and neutron stars. Phys. Rep. **411**, 325 (2005). https://doi.org/10.1016/j.physrep.2005.02.004
64. B.K. Agrawal, S.K. Dhiman, R. Kumar, Exploring the extended density-dependent Skyrme effective forces for normal and isospin-rich nuclei to neutron stars. Phys. Rev. C **73**, 034319 (2006). https://doi.org/10.1103/PhysRevC.73.034319
65. B.K. Agrawal, S. Shlomo, V.K. Au, Determination of the parameters of a Skyrme type effective interaction using the simulated annealing approach. Phys. Rev. C **72**, 014310 (2005). https://doi.org/10.1103/PhysRevC.72.014310
66. L.G. Cao, U. Lombardo, C.W. Shen et al., From Brueckner approach to Skyrme-type energy density functional. Phys. Rev. C **73**, 014313 (2006). https://doi.org/10.1103/PhysRevC.73.014313
67. L.W. Chen, C.M. Ko, B.A. Li et al., Density slope of the nuclear symmetry energy from the neutron skin thickness of heavy nuclei. Phys. Rev. C **82**, 024321 (2010). https://doi.org/10.1103/PhysRevC.82.024321
68. M. Rashdan, A Skyrme parametrization based on nuclear matter BHF calculations. Mod. Phys. Lett. A **15**, 1287 (2000). https://doi.org/10.1142/S0217732300001663
69. F. Tondeur, M. Brack, M. Farine et al., Static nuclear properties and the parametrisation of Skyrme forces. Nucl. Phys. A **420**, 297 (1984). https://doi.org/10.1016/0375-9474(84)90444-5
70. B.A. Brown, G. Shen, G.C. Hillhouse et al., Neutron skin deduced from antiprotonic atom data. Phys. Rev. C **76**, 034305 (2007). https://doi.org/10.1103/PhysRevC.76.034305
71. P.A.M. Guichon, H.H. Matevosyan, N. Sandulescu et al., Physical origin of density dependent forces of Skyrme type within the quark meson coupling model. Nucl. Phys. A **772**, 1 (2006). https://doi.org/10.1016/j.nuclphysa.2006.04.002
72. P. Klüpfel, P.-G. Reinhard, T.J. Bürvenich et al., Variations on a theme by Skyrme: a systematic study of adjustments of model parameters. Phys. Rev. C **79**, 034310 (2009). https://doi.org/10.1103/PhysRevC.79.034310
73. J.F. Berger, M. Girod, D. Gogny, Time-dependent quantum collective dynamics applied to nuclear fission. Comput. Phys. Commun. **63**, 365 (1991). https://doi.org/10.1016/0010-4655(91)90263-K
74. F. Chappert, M. Girod, S. Hilaire, Towards a new Gogny force parameterization: impact of the neutron matter equation of state. Phys. Lett. B **668**, 420 (2008). https://doi.org/10.1016/j.physletb.2008.09.017
75. S. Goriely, S. Hilaire, M. Girod et al., First Gogny–Hartree–Fock–Bogoliubov nuclear mass model. Phys. Rev. Lett. **102**, 242501 (2009). https://doi.org/10.1103/PhysRevLett.102.242501
76. A.M. Lane, Isobaric spin dependence of the optical potential and quasi-elastic (p, n) reactions. Nucl. Phys. **35**, 676 (1962). https://doi.org/10.1016/0029-5582(62)90153-0
77. L.W. Chen, B.J. Cai, C.M. Ko et al., Higher-order effects on the incompressibility of isospin asymmetric nuclear matter. Phys. Rev. C **80**, 014322 (2009). https://doi.org/10.1103/PhysRevC.80.014322